

Publisher: GSA
Journal: GEOL: Geology
DOI:10.1130/G37262.1

1 Links between arc volcanoes and porphyry-epithermal ore 2 deposits

3 **Olivier Nadeau¹, John Stix², and Anthony E. Williams-Jones²**

4 *¹Department of Earth and Environmental Sciences, University of Ottawa, Ottawa,
5 Ontario K1N 6N5, Canada*

6 *²Department of Earth and Planetary Sciences, McGill University, Montreal, Quebec H3A
7 0E8, Canada*

8 ABSTRACT

9 Porphyry and epithermal ore deposits, which are the products of magmatic
10 hydrothermal fluids, are intimately associated with volcanoes in continental and island
11 arcs above subduction zones, but the exact nature of this relationship has remained
12 enigmatic. Although metal deposition is usually thought to occur during the waning
13 stages of volcanism, numerous ore deposits have been demonstrated to be syn-volcanic.

14 Here we show how the formation of these deposits is tied to volcanic cycles. We relate
15 the chemical variations in vapors from Merapi volcano, Indonesia, to different stages of
16 its eruptive cycle. The chemical compositions of volcanic vapors from subduction zone
17 volcanoes are then compared globally to those of fluid inclusions from porphyry-
18 epithermal deposits. These data show that adiabatic decompression is the principal
19 control on mineralization. They also suggest that volcanic and sub-volcanic magmatic-
20 hydrothermal systems are under lithostatic pressure during quiescence but decompress
21 rapidly during injections of mafic magma and explosive eruptions. During quiescence,
22 the magma evolves through fractional crystallization and devolatilization, gradually

23 becoming oxidized and enriched in gold and other incompatible metals. Upon the
24 injection of sulfur-rich mafic magmas, subvolcanic intrusions brecciate the overlying
25 rocks, the systems are depressurized, the volcanoes erupt explosively, supercritical fluids
26 unmix into vapor and brine, and base metal sulfides precipitate.

27 **INTRODUCTION**

28 Magmatic-hydrothermal ore deposits form over periods ranging from thousands
29 to millions of years (Sillitoe, 2010), a generally shorter lifespan than that of arc volcanoes
30 which are thought to usually remain active for millions of years (Newhall et al., 2000).

31 Although the economic mineralization is usually considered to postdate volcanism
32 (Williams-Jones and Heinrich, 2005), numerous ore deposits have been shown to be
33 genetically associated with volcanism (Hattori and Keith, 2001) or even interrupted by
34 episodes of renewed magmatic activity (Maughan et al., 2002). Interestingly, the
35 injection of sulfur-rich mafic magmas into shallow porphyry stocks appears to trigger
36 explosive eruptions (Eichelberger, 1980) and generate ore deposits (Hattori and Keith,
37 2001). This paper reports data on the distribution of metals, sulfur and chlorine in
38 volcanic vapors collected at Merapi volcano during a phase of quiescent degassing in
39 2004 and after a large explosive eruption in 2006, and compares them to data reported for
40 volcanic vapors globally and for fluid inclusions from porphyry deposits. These data and
41 comparisons provide the first convincing evidence that injections of mafic magma (which
42 commonly coincide with explosive volcanic eruptions) are followed by decompression of
43 the magmatic hydrothermal system, inducing fluid phase separation, rapid cooling and
44 the deposition of porphyry and epithermal ores. In so doing they demonstrate the
45 important links between arc volcanism and porphyry-epithermal ore formation.

46 **METHODS**

47 Volcanic vapors were sampled by inserting silica tubes into fumaroles and
48 connecting the tubes to ice-trap condensers. The liquid that collected in the ice trap was
49 analyzed by ICP-MS, ICP-OES, INAA and IC. Sublimes from the vapors were
50 collected by inserting silica tubes into fumaroles immediately after the condensates were
51 sampled and waiting several days until sufficient solid had accumulated on the inner
52 walls of the tubes. Temperatures were measured along the tube centerlines using a
53 thermocouple. Aliquots of sublimes were mounted on polished sections for mineral
54 identification via EMPA and the remainder was analyzed using XRD.

55 **RESULTS**

56 **Vapor Compositions**

57 The concentrations of ligands (S-Cl) and metals (Au-Cu-Zn-Pb-Mo-Y-U) in
58 condensed vapor were normalized to Na to compensate for variations in density and thus
59 $f\text{H}_2\text{O}$ of the vapor (Fig. 1a). The vapors were enriched in S-Cl-Pb-Cu-Zn in 2006
60 (explosive) and enriched in Mo-Y-Au-U in 2004 (quiescent). In 2006, S and Cl
61 concentrations in the vapor ranged from 0.7 to 1.0 wt.% and 0.5–0.7 wt.%, respectively,
62 whereas they varied from 260 to 520 ppm and 890 to 3030 ppm, respectively, in 2004
63 (Table 1). Copper and Zn concentrations ranged from 0.16 to 0.28 ppm and 0.15 to 0.42
64 ppm, respectively, in 2006 and only 0.003 ppm and 0.06 to 0.15 ppm, respectively, in
65 2004. By contrast, concentrations of Mo only reached 0.6 ppb in 2006 compared to 4–20
66 ppb in 2004. The concentrations of Y were 0.7–4 ppb in 2004 and 0.4–0.5 ppb in 2006,
67 those of Au were 0.2–0.6 ppb in 2004 and 0.02 ppb in 2006, and those of U were 0.09–
68 0.34 ppb in 2004 and 0.06–0.08 ppb in 2006.

69 The concentrations of the REE were first normalized to Na and subsequently to
70 chondrite (McDonough and Sun, 1995) to allow comparison with subduction zone fluids
71 (Fig. 1b). The ‘doubly-normalized’ REE profiles all show LREE enrichment typical of
72 subduction zone fluids. The vapors from 2004 had higher total REE contents compared to
73 those from 2006. The concentrations of LILE and HFSE were first normalized to Na and
74 subsequently to MORB (McDonough and Sun, 1995) to evaluate fluid behavior (Fig. 1c).
75 All samples display gradual enrichment of progressively more incompatible elements,
76 except Ti, because it was compatible in titanomagnetite (Camus, 2000; Nadeau et al.,
77 2013). All incompatible elements are enriched in 2004 samples relative to those for 2006,
78 except for Zr and Hf in one sample.

79 **Sublimate Mineralogy and Redox State**

80 A variety of minerals precipitated from the vapors during cooling along the silica
81 tubes. In 2004, the mineral assemblage consisted of chlorides, sulfates and hydrated
82 sulfates, oxides and native elements, whereas the minerals comprised chlorides, sulfides,
83 arsenosulfides and native elements in 2006 (Fig. 2; Table DR1).

84 Iron precipitated in ilmenite and hematite in 2004 and in pyrite and smythite in
85 2006, Pb precipitated as anglesite in 2004 and as galena and tsugaruite ($Pb_4As_2S_7$) in
86 2006, and Bi, Zn-Cd precipitated as bismuthinite and wurtzite-greenockite in 2006. The
87 magmatic-hydrothermal system was thus relatively oxidized in 2004 and reduced in
88 2006.

89 **Magmatic Arc Fluids**

90 In order to expand our database beyond that of Merapi and to compare volcanic
91 vapors to ore fluids, we compiled published compositional data for 282 samples of vapor

92 condensates from 19 subduction zone stratovolcanoes (Table DR2) and 292 fluid
93 inclusion assemblages from seven major porphyry Cu ± Mo ± Au deposits (Table DR3)
94 (Fig. 3). These data are illustrated in violin plots showing median (black dot) and
95 interquartile range (black line) values as well as the total data distribution (gray envelope)
96 (see supplementary information). The volcanic vapors ranged in temperature from 85 °C
97 to 1020 °C, averaging 445 ± 216 °C (1σ), whereas the fluid inclusions were trapped at
98 temperatures from 220 °C to 771 °C or an average of 434 ± 130 °C (1σ). On average,
99 base metal concentrations in fluid inclusions from porphyry deposits are more than three
100 orders of magnitude higher than in volcanic vapors. Given their similar temperatures, and
101 experimental studies of metal solubility in aqueous fluids, the higher metal content of the
102 fluid inclusions is attributed to their higher fluid density and resulting higher capacity to
103 hydrate metal complexes. At constant density, metal solubility increases with increasing
104 temperature due to a corresponding increase in the partial pressure of H₂O, which
105 promotes the formation of metal complexes with high hydration numbers (e.g., Migdisov
106 et al., 2014). Increasing temperature, however, destabilizes metal complexes with high
107 hydration numbers, and a maximum solubility is reached when this effect outweighs that
108 of the increasing partial pressure of H₂O. In volcanic emissions, the Pb/Na ratio reaches a
109 maximum in fluids with temperatures of 400–600 °C, Zn/Na is greatest in fluids with
110 temperatures of 400–800 °C and Cu/Na and Au/Na have maxima in fluids with
111 temperatures of 200–400 °C. The use of Y as a proxy for the REE suggests that REE/Na
112 ratios are greatest in vapors with temperatures of 400–600 °C (Fig. 3a).
113 The Pb/Na, Zn/Na and Mo/Na ratios are much lower in fluid inclusions than in
114 volcanic vapors (Fig. 3b). This probably results from the preferential incorporation of Na

115 in alteration minerals precipitating from the fluid between the porphyry and the
116 fumaroles. By contrast, Cu/Na is higher in supercritical and vapor fluid inclusions and
117 lower in brines and volcanic vapors. However, the higher content of Cu in vapor
118 inclusions has been interpreted to result from post-entrapment diffusion of Cu toward the
119 vapor inclusions (Lerchbaumer and Audéat, 2012). The Cu/Na ratio is thus higher in
120 supercritical fluids than in brines, vapors and volcanic vapors, implying that Cu-bearing
121 minerals undergo largescale precipitation during the unmixing of supercritical fluids into
122 brine and vapor.

123 **DISCUSSION**

124 **Physical State of the Volatile Phase**

125 An important difference between porphyry fluids and volcanic vapors is their
126 physical state. Magmatic volatiles exsolved at pressures and temperatures greater than
127 those of the critical point, i.e., porphyry fluids at depth, are in a supercritical state. When
128 supercritical fluids ascend, they may reach the critical point and unmix into liquid and
129 vapor. Upon unmixing, Cl preferentially partitions into the liquid forming brine (Bodnar
130 et al., 1985) whereas S partitions preferentially into the vapor that is ultimately emitted as
131 a volcanic gas (Simon and Ripley, 2011; Nadeau et al., 2013).

132 Pressure has a major impact on the physical state of magmatic hydrothermal
133 fluids because decreasing pressure may lead to phase separation. It is possible to relate
134 the pressure at which supercritical fluids unmix into brine and vapor to a critical depth,
135 by assuming lithostatic and hydrostatic pressure gradients. According to experimental
136 studies in the H₂O-NaCl system, for a magmatic fluid at 1000 °C and 5–10 wt. % NaCl_{eq}
137 (Zajacz et al., 2008), the critical depth is 5 km under a lithostatic pressure gradient and 15

138 km under a hydrostatic pressure gradient (Driesner and Heinrich, 2007). The addition of
139 CO₂ and sulfur species to the system will increase this critical depth, but phase
140 relationships in the COHS-NaCl system are not sufficiently known to quantify this effect
141 (Webster and Mandeville, 2007).

142 **Variations in Sulfur and Chlorine**

143 Porphyry-type deposits have greater contents of sulfur than of the base and
144 precious metals for which they are exploited. At Merapi, volcanic vapors were highly
145 enriched in S following the explosive eruption of 2006 compared to volcanic vapors that
146 were quiescently degassed in 2004 (Table 1). The total concentration of S in vapor
147 condensates was 6730 and 10,580 ppm in 2006, and 260 and 520 ppm in 2004; the higher
148 concentration of 2006 was attributed to the injection of sulfide melt-saturated mafic
149 magma in that year (Nadeau et al., 2010). Chlorine was present in significant
150 concentrations in volcanic vapors released from Merapi in both 2004 and 2006, but its
151 concentration varied much less than that of sulfur between periods of quiescence and
152 eruption.

153 **Redox Conditions**

154 During periods of quiescent degassing, magma becomes oxidized due to the
155 preferential incorporation of Fe²⁺ in minerals (Kelley and Cottrell, 2012) and fluids (Bell
156 and Simon, 2011) and preferential degassing of H₂ relative to O₂ during H₂O
157 disproportionation (Mathez, 1984). Although primitive arc magmas are usually
158 considered to be oxidized ($fO_2 \geq$ FMQ+2; Mungall, 2002), the deep mafic magmas
159 feeding Merapi were sufficiently reduced, with fO_2 at or near FMQ (Jugo, 2009), to
160 exsolve an immiscible sulfide melt (Nadeau et al., 2010) and an aqueous fluid that

161 ultimately precipitated sulfides (Fig. 2b). Such immiscible sulfide melt inclusions also
162 have been observed at other arc volcanoes and in porphyry Cu deposits (Larocque et al.,
163 2000), suggesting that deep mafic feeders commonly may be less oxidized than shallower
164 porphyry stocks.

165 Variations in the degree of oxidation of magmas and fluids have an important
166 impact on metal transport characteristics. Highly oxidized magmas lack sulfides that
167 could scavenge chalcophile and siderophile metals from magmatic-hydrothermal
168 systems. In contrast, S-rich, reduced magmas may exsolve chalcophile element-rich
169 immiscible sulfide melts that, in turn, can be subsequently dissolved in magmatic
170 hydrothermal fluids (Nadeau et al., 2010; Mungall et al., 2015). High oxidation states of
171 hydrothermal fluids lead to low H₂S/SO₂ ratios, inhibiting the solubility of metals that are
172 dissolved dominantly as bisulfide complexes (Zezin et al., 2011) but enhancing the
173 capacity of the melt to transport sulfur as SO₄²⁻ (Jugo, 2009).

174 **Metallogenesis of Porphyry-Type Deposits**

175 We propose that porphyry-epithermal systems evolve by cycling through periods
176 of volcanic quiescent degassing dominated by fractional crystallization and volatile
177 exsolution, and periods of explosive activity triggered by injection of mafic magmas (Fig.
178 4). According to this hypothesis, quiescently devolatilizing magmas evolve under
179 lithostatic pressure gradients to relatively shallow depths (the critical depth is 5 km in the
180 H₂O-NaCl system; Driesner and Heinrich, 2007). Incompatible metals such as Au, Mo,
181 REE, HFSE and LILE are gradually enriched in the magmas and fluids and deposited in
182 these relatively oxidizing environments. Injections of less oxidized mafic magmas open
183 up the systems and abruptly decrease the confining pressures to values closer to the

184 hydrostatic gradient, thereby displacing the critical depth to deeper levels (15 km in the
185 H₂O-NaCl system; Driesner and Heinrich, 2007). Regional tectonic earthquakes, such as
186 that which occurred near Merapi during the eruption of 2006, also may enhance the
187 pressure regime transition by opening the systems. Although experimental studies in the
188 H₂O-NaCl system suggest a critical depth of 15 km under a hydrostatic pressure gradient,
189 a study of rock rheology suggests that a hydrostatic regime would be difficult to maintain
190 at depths greater than ~5–10 km (Sibson, 1992). Hence the pressure regime at this stage
191 may lie between lithostatic and hydrostatic. Upon depressurization, sulfur partitions
192 preferentially into the vapor which rises and expands, whereas chlorine remains in the
193 brine that ponds beneath the volcano.

194 After the injection of mafic magma, Cu bonds with S to precipitate as a sulfide
195 mineral under the combined effects of decompression and expansion of the hydrated
196 metal complexes. The precipitation of Zn and Pb, which are also enriched in the
197 hydrothermal system after rock failure and decompression, is not as abrupt as that of Cu
198 (Fig. 3b) as these metals form stronger bonds with Cl. Their precipitation in sulfide
199 minerals is thus delayed relative to Cu. After explosive eruptions which typically last
200 several months and contribute to fracturing and brecciating rocks at progressively greater
201 depths, the magmas evolve by fractional crystallization, gradually becoming more
202 oxidized and enriched in incompatible elements. The hydrothermal system seals itself by
203 precipitation of minerals along fractures and in breccias under the weight of the rock
204 column, with pressure returning to lithostatic levels. The ability of the fluid to dissolve
205 metals gradually increases until the next explosive eruption (or rock failure at depth),
206 typically a few years later.

207 **CONCLUSIONS AND IMPLICATIONS**

208 Although economic mineralization is usually thought to postdate volcanism
209 (Williams-Jones and Heinrich, 2005), numerous ore deposits have been shown to be
210 genetically associated with volcanism (Hattori and Keith, 2001). In this paper, we have
211 related variations in the composition of volcanic vapors from Merapi volcano to different
212 stages of its eruptive cycle and compared these compositions to those of volcanic vapors
213 from other subduction zone volcanoes and porphyry-hosted fluid inclusions. These data
214 provide the first convincing evidence that injections of mafic magma (which commonly
215 coincide with explosive volcanic eruptions) are followed by decompression of the
216 magmatic hydrothermal system, inducing fluid phase separation, rapid cooling and the
217 deposition of porphyry and epithermal ores. In so doing they demonstrate that
218 decompression is the principal control on mineralization, and that pressure in the systems
219 transforms abruptly from lithostatic during quiescence to hydrostatic during and
220 immediately after an explosive eruption (rock failure at depth). During quiescence,
221 magmatic-hydrothermal systems evolve through crystallization and devolatilization,
222 gradually becoming oxidized and enriched in gold and other incompatible metals. Upon
223 injection of mafic magmas, they are depressurized, supercritical fluids unmix into vapor
224 and brine, temperature drops, base metal sulfides precipitate at depth and volcanoes erupt
225 explosively.

226 **ACKNOWLEDGMENTS**

227 This research was made possible by NSERC Discovery grants to AEWJ and JS,
228 and an NSERC PhD scholarship to ON. We thank F. Gaillard and two anonymous
229 reviewers for their constructive comments.

230 **REFERENCES CITED**

- 231 Bell, A.S. and Simon, A., 2011. Experimental evidence for the alteration of the Fe^{3+} /
232 ΣFe of silicate melt caused by the degassing of chlorine-bearing aqueous volatiles.
233 Geology, v. 39, p. 499–502, doi: 10.1130/G31828.1
- 234 Bodnar, R.J., Burnham, C.W., and Stern, S.M., 1985, Synthetic fluid inclusions in
235 natural quartz; III, Determination of phase equilibrium properties in the system H₂O-
236 NaCl to 1000 degrees C and 1500 bars: Geochimica et Cosmochimica Acta, v. 49,
237 p. 1861–1873, doi:10.1016/0016-7037(85)90081-X.
- 238 Camus, G., Gourgaud, A., Mossand-Berthommier, P. C., Vincent, P. M., 2000. Merapi
239 (central Java, Indonesia); an outline of the structural and magmatological evolution,
240 with a special emphasis to the major pyroclastic events. Journal of Volcanology and
241 Geothermal Research, v. 100, p. 139–163, doi:10.1016/S0377-0273(00)00135-9
- 242 Driesner, T., and Heinrich, C.A., 2007, The system H₂O-NaCl; Part I, Correlation
243 formulae for phase relations in temperature-pressure-composition space from 0 to
244 1000 degrees C, 0 to 5000 bar, and 0 to 1 X_{NaCl}: Geochimica et Cosmochimica Acta,
245 v. 71, p. 4880–4901, doi:10.1016/j.gca.2006.01.033.
- 246 Eichelberger, J.C., 1980, Vesiculation of mafic magma during replenishment of silicic
247 magma reservoirs: Nature, v. 288, p. 446–450, doi:10.1038/288446a0.
- 248 Hattori, K.H., and Keith, J.D., 2001, Contribution of mafic melt to porphyry copper
249 mineralization; evidence from Mount Pinatubo, Philippines, and Bingham Canyon,
250 Utah, USA: Mineralium Deposita, v. 36, p. 799–806, doi:10.1007/s001260100209.
- 251 Jugo, P.J., 2009, Sulfur content at sulfide saturation in oxidized magmas: Geology, v. 37,
252 p. 415–418, doi:10.1130/G25527A.1.

- 253 Kelley, K.A., and Cottrell, E., 2012, The influence of magmatic differentiation on the
254 oxidation state of Fe in a basaltic arc magma: *Earth and Planetary Science Letters*,
255 v. 329–330, p. 109–121, doi:10.1016/j.epsl.2012.02.010.
- 256 Larocque, A.C.L., Stimac, J.A., Keith, J.D., and Huminicki, M.A.E., 2000, Evidence for
257 open-system behavior in immiscible Fe-S-O liquids in silicate magmas; implications
258 for contributions of metals and sulfur to ore-forming fields: *Canadian Mineralogist*,
259 v. 38, p. 1233–1249, doi:10.2113/gscanmin.38.5.1233.
- 260 Lerchbaumer, L., and Audétat, A., 2012, High Cu concentrations in vapor-type fluid
261 inclusions: An artifact?: *Geochimica et Cosmochimica Acta*, v. 88, p. 255–274,
262 doi:10.1016/j.gca.2012.04.033.
- 263 Mathez, E.A., 1984, Influence of degassing on oxidation states of basaltic magmas:
264 *Nature*, v. 310, p. 371–375, doi:10.1038/310371a0.
- 265 Maughan, D.T., Keith, J.D., Christiansen, E.H., Pulsipher, T., Hattori, K., and Evans, N.,
266 2002, Contributions from mafic alkaline magmas to the Bingham porphyry Cu-Au-
267 Mo deposit, Utah, USA: *Mineralium Deposita*, v. 37, p. 14–37, doi:10.1007/s00126-
268 001-0228-5.
- 269 McDonough, W.F., and Sun, S., 1995, The composition of the Earth: *Chemical Geology*,
270 v. 120, p. 223–253, doi:10.1016/0009-2541(94)00140-4.
- 271 Migdisov, A., Bychkov, A.Y., Williams-Jones, A.E., and van Hinsberg, V.J., 2014, A
272 predictive model for the transport of copper by HCl-bearing water vapour in ore-
273 forming magmatic-hydrothermal systems; implications for copper porphyry ore
274 formation: *Geochimica et Cosmochimica Acta*, v. 129, p. 33–53,
275 doi:10.1016/j.gca.2013.12.024.

- 276 Mungall, J.E., 2002. Roasting the mantle; slab melting and the genesis of major Au and
277 Au-rich Cu deposits. *Geology*, v. 30, p. 915–918, doi: 10.1130/0091-
278 7613(2002)030<0915:RTMSMA>2.0.CO;2
- 279 Mungall, J.E., Brenan, J.M., Godel, B., Barnes, J.J., and Gaillard, F., 2015, Transport of
280 metals and sulphur in magmas by flotation of sulphide melt on vapour bubbles:
281 *Nature Geoscience*, v. 8, p. 216–219, doi:10.1038/ngeo2373.
- 282 Nadeau, O., Williams-Jones, A.E., and Stix, J., 2010, Sulfide magma as a source of
283 metals in arc-related magmatic hydrothermal ore fluids: *Nature Geoscience*, v. 3,
284 p. 501–505, doi:10.1038/ngeo899.
- 285 Nadeau, O., Williams-Jones, A.E., and Stix, J., 2013, Magmatic-Hydrothermal Evolution
286 and Devolatilization Beneath Merapi Volcano, Indonesia: *Journal of Volcanology*
287 and Geothermal Research, v. 261, p. 50–68, doi:10.1016/j.jvolgeores.2013.04.006.
- 288 Newhall, C.G., Bronto, S., Alloway, B.V., Banks, N.G., Bahar, I., del Marmol, M.A.,
289 Hadisantono, R.D., Holcomb, R.T., McGeehin, J.P., Miksic, J.N., Rubin, Meyer,
290 Sayudi, D.S., Sukhyar, R., Andreastuti, S.D., Tilling, R.I., Torley, R., Trimble, D.A.,
291 Wirakusumah, A.D., 2000, 10,000 years of explosive eruptions of Merapi Volcano,
292 central Java; archaeological and modern implications: *Journal of Volcanology and*
293 *Geothermal Research*, v. 100, p. 9–50.
- 294 Sibson, R.H., 1992, Fault-valve behavior and the hydrostatic-lithostatic fluid pressure
295 interface: *Earth-Science Reviews*, v. 32, p. 141–144, doi:10.1016/0012-
296 8252(92)90019-P.
- 297 Sillitoe, R.H., 2010, Porphyry copper systems: *Economic Geology and the Bulletin of the*
298 *Society of Economic Geologists*, v. 105, p. 3–41, doi:10.2113/gsecongeo.105.1.3.

- 299 Simon, A.C., and Ripley, E.M., 2011, The role of magmatic sulfur in the formation of ore
300 deposits: *Reviews in Mineralogy and Geochemistry*, v. 73, p. 513–578,
301 doi:10.2138/rmg.2011.73.16.
- 302 Webster, J.D., and Mandeville, C.W., 2007, Fluid immiscibility in volcanic
303 environments: *Reviews in Mineralogy and Geochemistry*, v. 65, p. 313–362,
304 doi:10.2138/rmg.2007.65.10.
- 305 Williams-Jones, A.E., and Heinrich, C.A., 2005, Vapor transport of metals and the
306 formation of magmatic-hydrothermal ore deposits: *Economic Geology and the*
307 *Bulletin of the Society of Economic Geologists*, v. 100, p. 1287–1312,
308 doi:10.2113/gsecongeo.100.7.1287.
- 309 Zajacz, Z., Halter, W.E., Pettke, T., and Guillong, M., 2008, Determination of fluid/melt
310 partition coefficients by LA-ICPMS analysis of co-existing fluid and silicate melt
311 inclusions; controls on element partitioning: *Geochimica et Cosmochimica Acta*,
312 v. 72, p. 2169–2197, doi:10.1016/j.gca.2008.01.034.
- 313 Zezin, D.Y., Migdisov, A.A., and Williams-Jones, A.E., 2011, The solubility of gold in
314 H₂O-H₂S vapour at elevated temperature and pressure: *Geochimica et Cosmochimica*
315 *Acta*, v. 75, p. 5140–5153, doi:10.1016/j.gca.2011.06.027.
- 316
- 317 FIGURE CAPTIONS
- 318
- 319 Figure 1. Compositions of condensed vapors from Merapi in 2004–2006. Elements are
320 normalized to Na (a) and to chondrite (b) or MORB (c) (McDonough and Sun, 1995).
321 The gray envelopes represent all data from Merapi.

322

323 Figure 2. Mineralogy of volcanic vapor sublimes from Merapi in 2004–2006.

324

325 Figure 3. Compositions of volcanic vapor condensates (a) and comparison of fluid
326 inclusion and vapor condensate compositions (b) from selected arc volcanoes and
327 porphyry deposits. See supplementary information for references.

328

329 Figure 4. Schematic model showing the evolution of porphyry systems based on Merapi
330 volcano, Indonesia.

331

332 ¹GSA Data Repository item 2015xxx, xxxxxxxx, is available online at
333 www.geosociety.org/pubs/ft2015.htm, or on request from editing@geosociety.org or
334 Documents Secretary, GSA, P.O. Box 9140, Boulder, CO 80301, USA.

335

336

337

338

339

340

341

342

343

344

345

346

347

348

349

TABLE 1. COMPOSITIONS OF CONDENSED VOLCANIC VAPORS FROM MERAPI IN 2004–2006.

Year	Sample	Na	S	Cl	Ti	Cu	Zn	Sr	Y	Zr	Mo	Ba	La	Ce	Pr	Nd
2004	M4W1	3.43	263	3030	0.40		0.150	0.075	0.0039	0.0121	0.0200	0.281	0.0032	0.00718	0.00084	0.00365
2004	M4W3	0.60	520	893	0.21	0.003	0.060	0.015	0.0007	0.0048	0.0040	0.11	0.00078	0.0014	0.00015	0.00065
2006	M6W1	2.31	6733	4849	0.05	0.161	0.420	0.020	0.0004	0.0222		0.0342	0.00023	0.001862	0.000177	0.00072
2006	M6W2	1.21	10579	7193	0.05	0.279	0.150	0.019	0.0005	0.0114	0.0006	0.0555	0.000928	0.001798	0.000221	0.000813

Year	Sample	Sm	Eu	Gd	Tb	Dy	Ho	Er	Tm	Yb	Lu	Hf	Ta	Au	Pb	U
2004	M4W1	0.00089	0.00024	0.00095	0.00014	0.00073	0.00015	0.00041	0.00006	0.00041	0.00006	0.00031	0.00035	0.00060	1.41000	0.00034
2004	M4W3	0.00015	0.00006	0.00013	0.00003	0.00011	0.00003	0.00007		0.00008	0.00001	0.00012	0.00011	0.00020	0.07000	0.00009
2006	M6W1	0.00019	0.00003	0.00009	0.00001	0.00009	0.00002	0.00008	0.00000	0.00005		0.00049	0.00003		8.53000	0.00006
2006	M6W2	0.00020	0.00005	0.00014	0.00007	0.00013	0.00002	0.00009	0.00002	0.00005	0.00001	0.00028	0.00003	0.00002	8.01000	0.00008

350

Figure 1

Click here to download Figure Fig-1-condensates.jpg

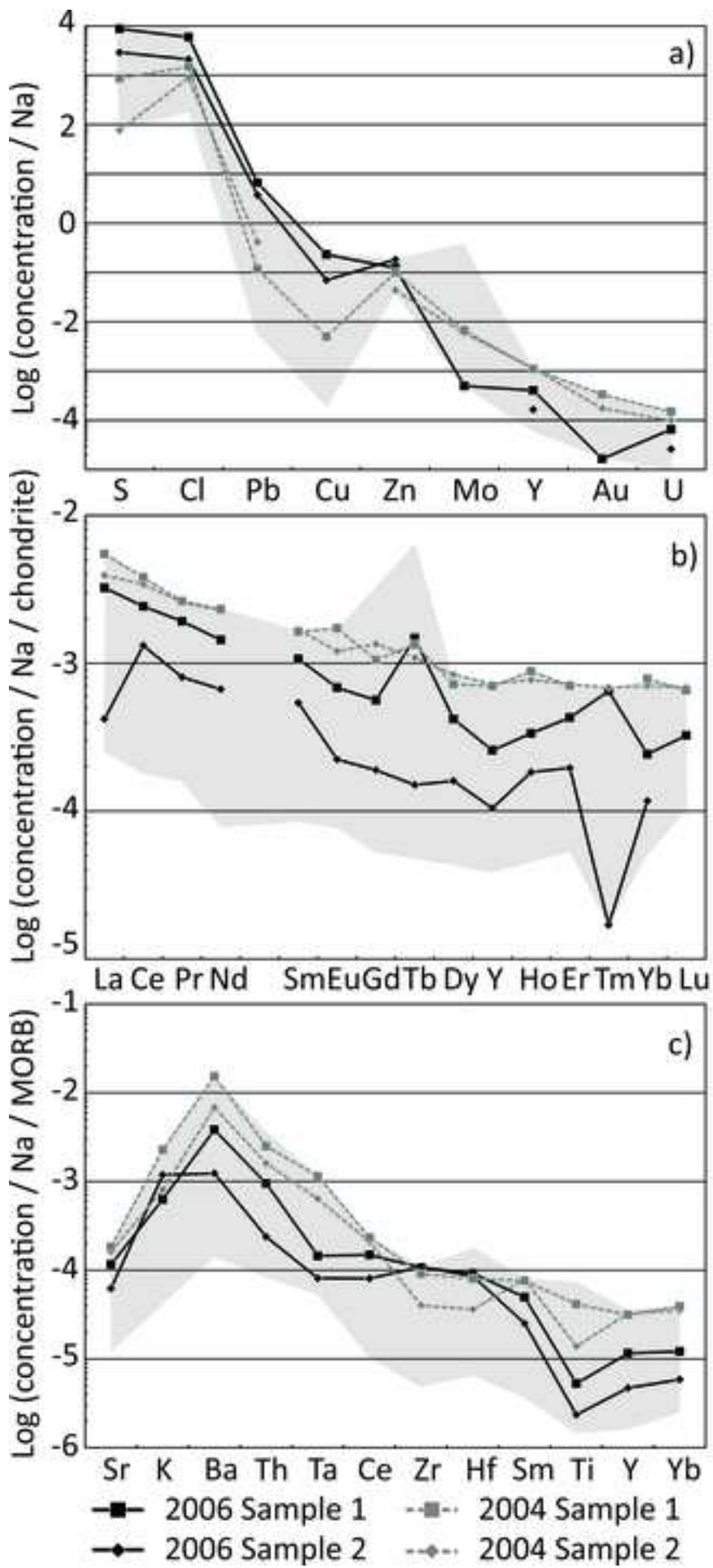


Figure 2

Click here to download Figure Fig-2-sublimates.jpg

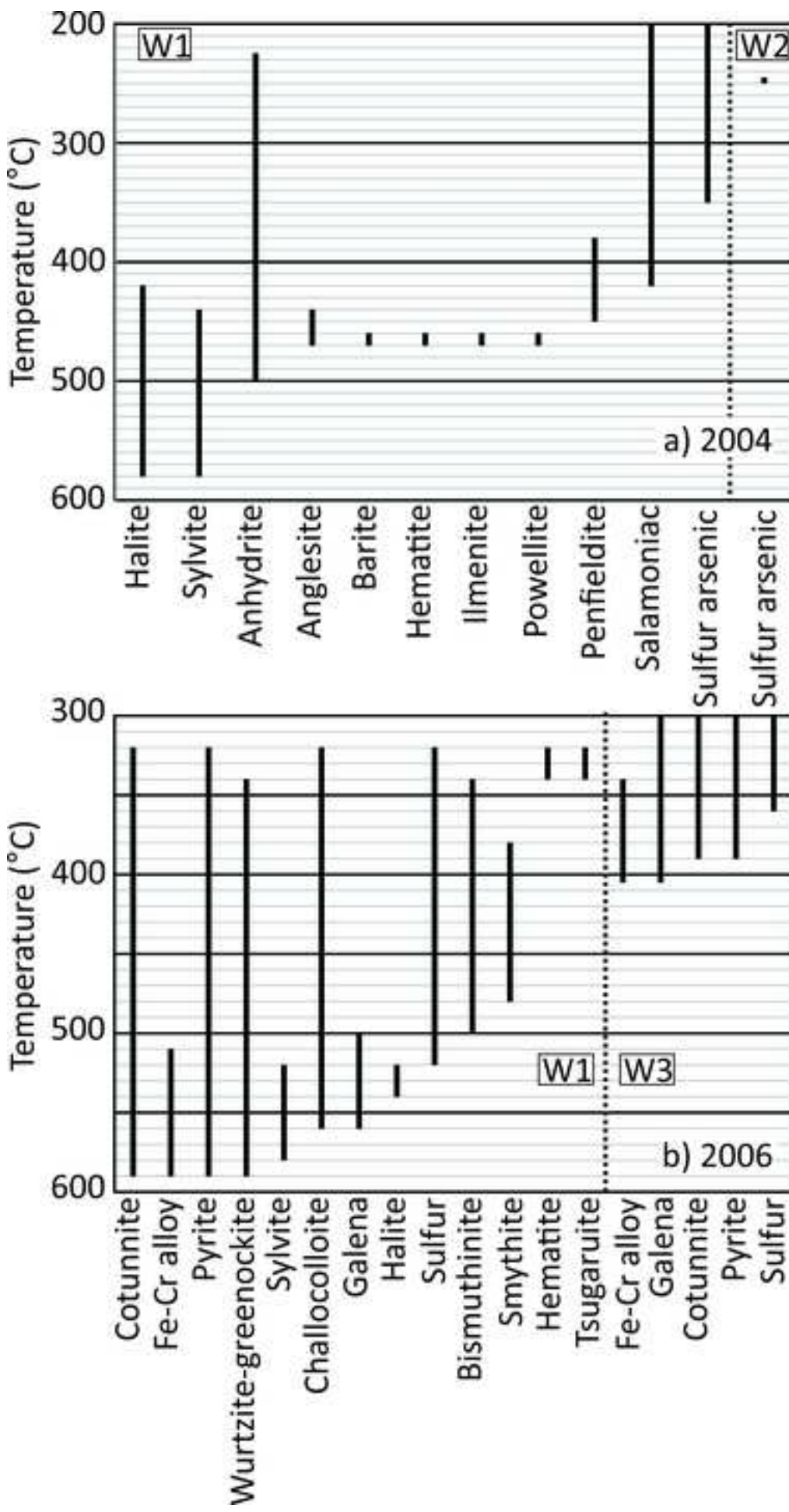


Figure 3

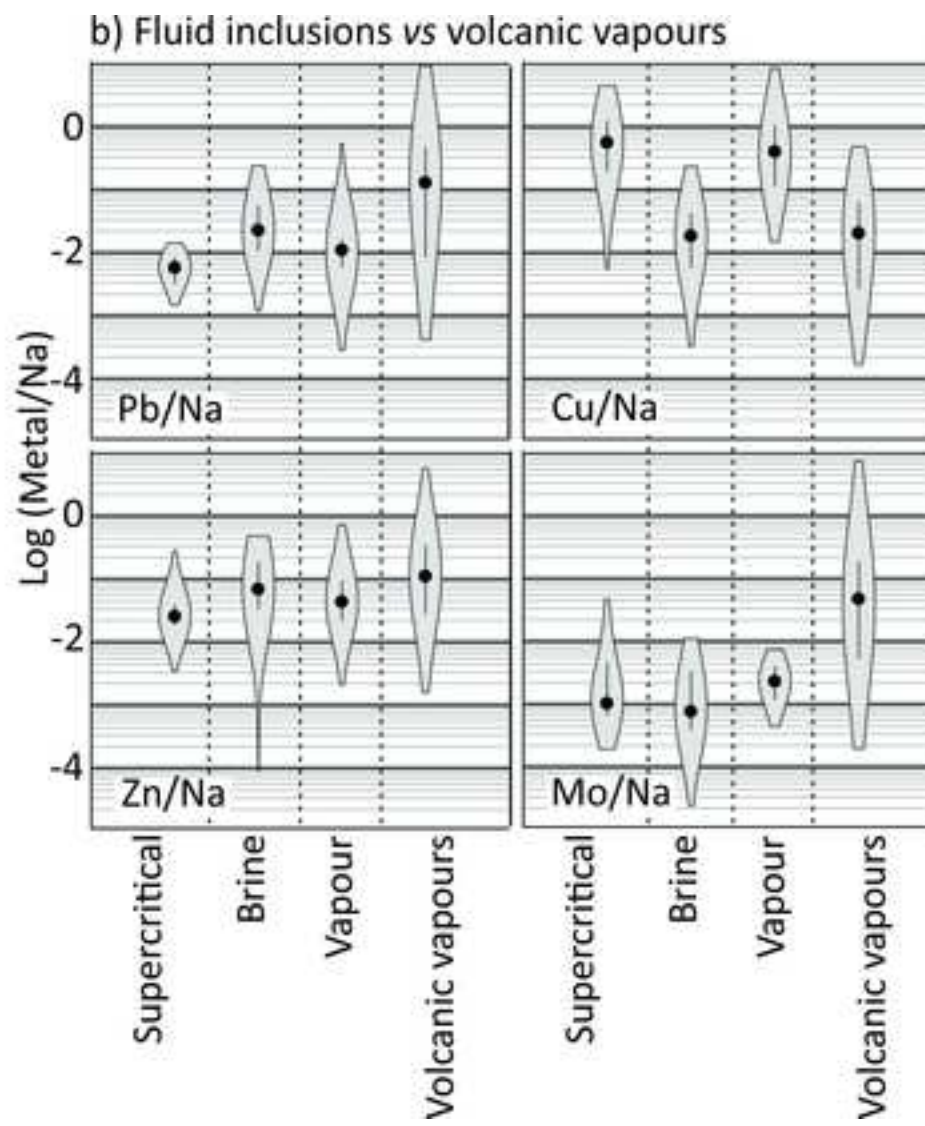
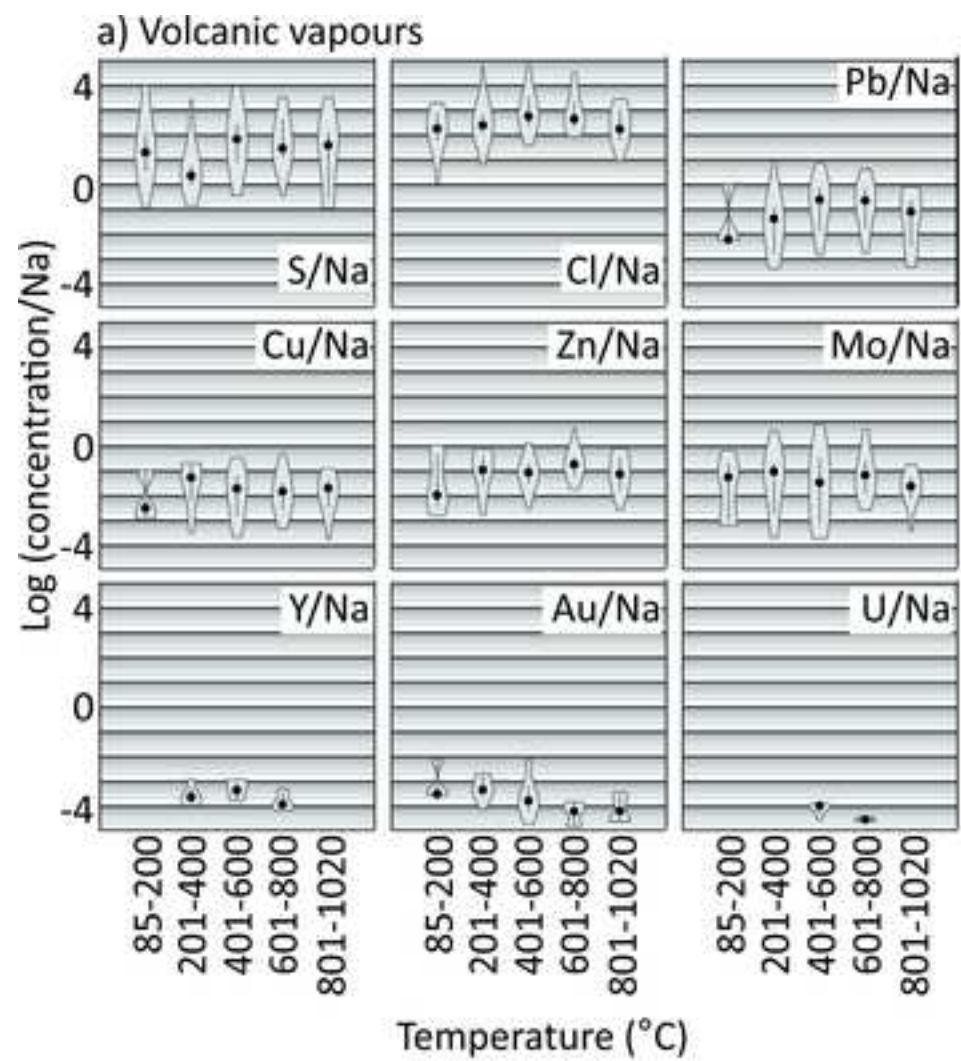
[Click here to download Figure Fig-3-Condensates-vs-flincs.jpg](#)


Figure 4

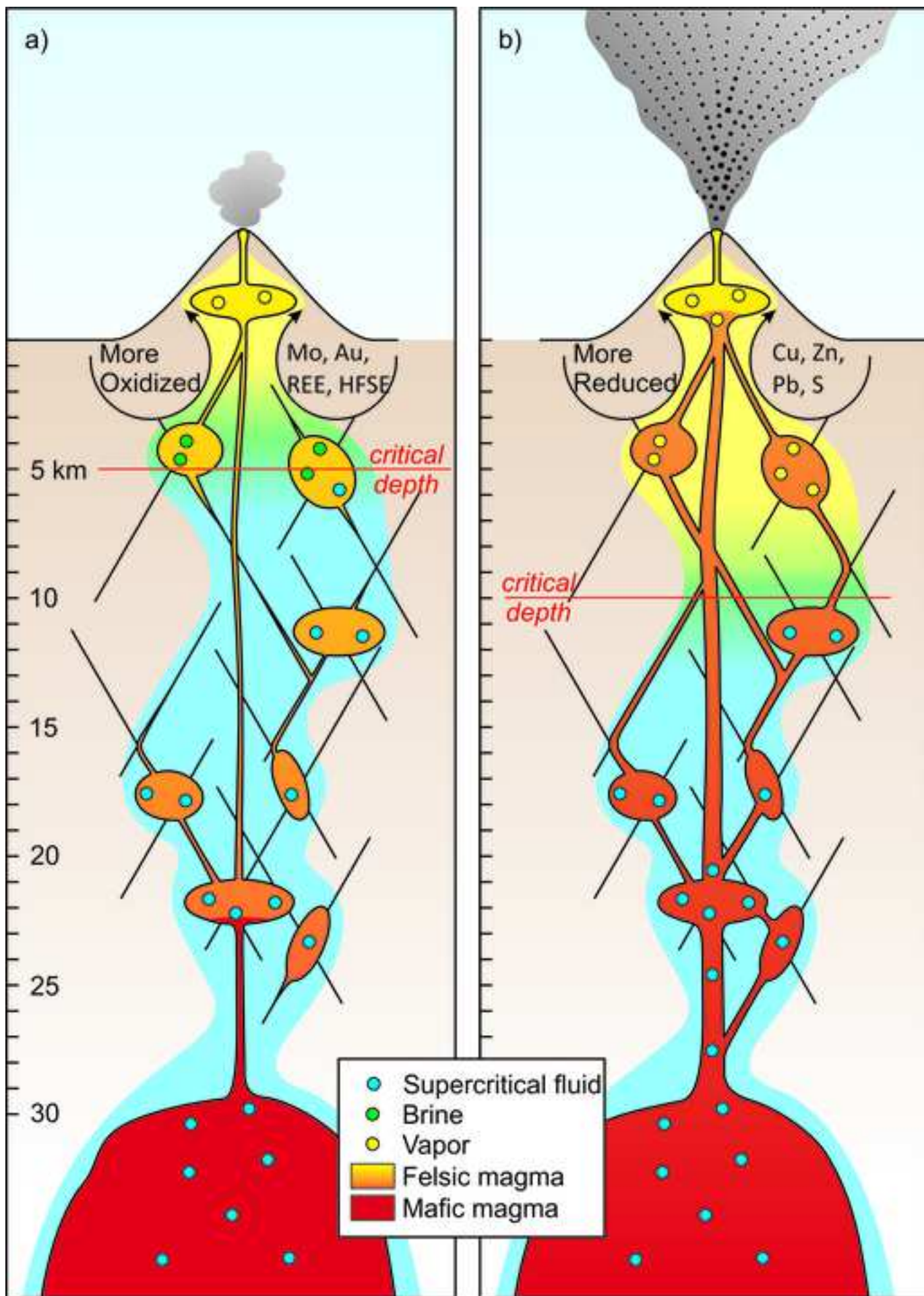
[Click here to download Figure Fig-4-cartoon.jpg](#)

Table 1

Year	Sample	Na	S	Cl	Ti	Cu	Zn	Sr	Y	Zr	Mo	Ba	La	Ce	Pr	Nd
2004	M4W1	3.43	263	3030	0.40		0.150	0.075	0.0039	0.0121	0.0200	0.281	0.0032	0.00718	0.00084	0.00365
2004	M4W3	0.60	520	893	0.21	0.003	0.060	0.015	0.0007	0.0048	0.0040	0.11	0.00078	0.0014	0.00015	0.00065
2006	M6W1	2.31	6733	4849	0.05	0.161	0.420	0.020	0.0004	0.0222		0.0342	0.00023	0.001862	0.000177	0.00072
2006	M6W2	1.21	10579	7193	0.05	0.279	0.150	0.019	0.0005	0.0114	0.0006	0.0555	0.000928	0.001798	0.000221	0.000813
Year	Sample	Sm	Eu	Gd	Tb	Dy	Ho	Er	Tm	Yb	Lu	Hf	Ta	Au	Pb	U
2004	M4W1	0.00089	0.00024	0.00095	0.00014	0.00073	0.00015	0.00041	0.00006	0.00041	0.00006	0.00031	0.00035	0.00060	1.41000	0.00034
2004	M4W3	0.00015	0.00006	0.00013	0.00003	0.00011	0.00003	0.00007		0.00008	0.00001	0.00012	0.00011	0.00020	0.07000	0.00009
2006	M6W1	0.00019	0.00003	0.00009	0.00001	0.00009	0.00002	0.00008	0.00000	0.00005		0.00049	0.00003		8.53000	0.00006
2006	M6W2	0.00020	0.00005	0.00014	0.00007	0.00013	0.00002	0.00009	0.00002	0.00005	0.00001	0.00028	0.00003	0.00002	8.01000	0.00008

Volcanic Processes and the Genesis of Porphyry and Epithermal Ore Deposits

Olivier Nadeau¹, John Stix² and Anthony E. Williams-Jones²

¹ Department of Earth and Environmental Sciences, University of Ottawa, Ottawa (Ontario), K1N 6N5, Canada

² Department of Earth and Planetary Sciences, McGill University, Montreal (Quebec), H3A 0E8, Canada

Supplementary Information

Geological Context

Merapi volcano was most active within the last 40,000 years (Camus et al., 2000). Since the beginning of the 20th century, Merapi has alternated between periods of quiescent degassing and lava dome growth and occasional collapse, typically lasting a few years, and periods of explosive activity, with St-Vincent - type explosions, pyroclastic flows and surges, typically lasting several months. From September 2002 to March 2006, the volcano was in a phase of quiescent degassing. From March to July 2006, it went through a phase of explosive activity, with its plume reaching an altitude of 3.7 km and erupting about 1.07×10^{10} kg of rock (Ratdomopurbo et al., 2013). On May 27th 2006, a magnitude 6.3 earthquake occurred about 50 km SW of Merapi at a depth of about 10 km, resulting in a three-fold increase of volcanic activity (Global Volcanism Program of the National Museum of Natural History – Smithsonian Institution (GVP); United States Geological Survey, consulted online in June 2015). From July 2006 and until October 2010, it went back to a phase of quiescence. In 2010, the volcano had its greatest eruption since 1872. From October to November 2010, Merapi erupted about 3.1×10^{11} kg of rock and degassed about 0.44×10^9 kg of SO₂ (GVP; Surono et al., 2012). Although the initial explosion occurred 19 hours after a magnitude 7.7 earthquake 1200 km NW of Merapi, any links between this seismic event and the major eruption of 2010 are difficult to prove. Volcanic vapours at Merapi emanate from distinct fumarole fields. Gendol was the highest temperature fumarole field, with temperature reaching up to 900°C (Le Guern, 1979), until it was destroyed by the eruption in 2006. Woro was a lower temperature fumarole field, reaching up to 710°C (Le Guern et al., 1982), until it was destroyed by the 2010 eruption. In this paper we used only the volcanic vapour data from Woro as they were the only dataset that could be compared between 2004 and 2006 and because vapours from distinct fumarole fields cannot be compared directly.

Supplementary Methods

Condensates of volcanic vapor

Volcanic vapours were sampled by inserting meter-long fused silica tubes into fumaroles and connecting the quartz tubes to condensers filled with ice and pumping the vapour slowly through the condenser using a hand-held pump. The liquid that collected in the condenser was stored in Teflon bottles and analyzed at Actlabs Inc., Canada, by a combination of inductively coupled plasma mass spectrometry (ICP-MS), ICP optical emission spectrometry (OES), neutron activation (INAA) and ion chromatography.

Sublimes of volcanic vapor

The sampling of vapor condensates was complemented by inserting meter-long, fused silica tubes into the fumaroles immediately after the condensates had been collected and waiting until sufficient solid had precipitated on the inner walls of the tubes (Le Guern et al., 1982). In 2004, tubes were inserted for periods varying between four and six days. In 2006, tubes were in place for a period of 22 days. The sampling was done during the dry season to avoid dissolution and redistribution of sublimates by rain. Temperatures were measured along the tube centerlines at 10 cm intervals using a meter-long thermocouple and the tubes were subsequently cut into sections representing increments of 10 to 20°C. The sublimates were scraped off and a fraction of each sublimate was mounted on a glass slide and polished. As several of the sublimate phases are water soluble (e.g., halite and sylvite), the polishing agent (aluminium oxide or diamond powder) was suspended in alcohol rather than water. The phases in the polished sections were analysed chemically using a JEOL JXA-8900L electron microprobe (EMPA) at McGill University. A second fraction of sublimate was scanned using a Siemens D500 X-ray diffractometer equipped with a Co tube and a Si detector at the Université du Québec à Montréal. The diffraction patterns were analyzed using Jade software at McGill University for identification of major phases.

Supplementary Tables

Table S1. Mineralogy and temperature distribution of of volcanic vapour sublimates collected from Merapi volcano in 2004-2006.

Table S2. Compilation of volcanic vapour condensates

A total of 282 samples of vapour condensates from subduction zone stratovolcanoes with trace element concentrations were compiled from the literature (Fig. 2). Data were taken from Arenal, Costa Rica (Stoiber and Rose, 1970), Augustine, Alaska (Symonds et al., 1990), Cerro Negro, Nicaragua (Gummel, 1987; Stoiber and Rose, 1970), Colima, Mexico (Taran et al., 2001), Fuego, Guatemala (Stoiber and Rose, 1970), Izalco, El Salvador (Stoiber and Rose, 1970), Kawa Ijen, Indonesia (Berlo et al., 2014), Kudryavy, Russia (Wahrenberger et al., 2002; Taran et al., 1995), Masaya, Nicaragua (Gummel, 1987), Merapi, Indonesia (this research; Symonds et al., 1987), Momotombo, Nicaragua (Gummel, 1987), Mutnovsky, Kamchatka (Zelensky et al., 2005), New Tolbachik, Kamchatka (Menyailov and Nikitina, 1980), Pacaya, Guatemala (Stoiber and Rose, 1970), Poas, Costa Rica (Gummel, 1987), Santiagito, Guatemala (Stoiber and Rose, 1970), Satsuma Iwojima, Japan (Hedenquist et al., 1994), Showa Shinzan, Japan (Oana, 1962; Mizutani, 1970; Symonds et al., 1996) and St-Helens, USA (Bernard et al., 1990). The concentrations of S, Cl, Pb, Cu, Zn, Mo, Y, Au and U were normalized to Na to neutralise the effect of dilution by H₂O. The concentration of these elements did not show any correlation with the silica content nor with the alkalinity of the associated volcanic rocks. Conversely, a correlation was observed between their composition and temperature. The samples were thus separated into five temperature groups, i.e., 85-200°C (n=23), 201-400°C (n=109), 401-600°C (n=55), 601-800°C (n=44) and 801-1020°C (n=19). These results are reported in “violin plots”, using NCSS statistical software, showing the median (black dot), the interquartile range (central vertical line extending from the 25th to 75th percentile) and the total distribution (gray envelopes; width representing the amount of data).

Most of the violin plots show normal distributions, with medians near the centres of the interquartile bars and the latter approximately in the middle of the total distribution, except for some plots of the low temperature group with abnormal distributions, due to limited data. Uranium, Y, and Au to a lesser extent, also have limited data and show a limited temperature distribution and inconsistent statistical values. Sulphur and Cl have the highest concentrations of the elements in the volcanic vapour

condensates other than H and O. Concentrations of S range from 2 ppm to 2.7 wt.% and Cl from 10 ppm to 6.6 wt.%, values which are significantly higher than those of the base metals (Pb-Cu-Zn-Mo), which vary between 0.01 ppb and 21.9 ppm, and trace metals (REE, Au, U) which vary between 0.001 ppb and 0.22 ppm (Gemmel, 1987).

The temperature distribution of the volatile and metallic elements results in convex-upward patterns with maxima at intermediate values (usually around 400-800°C) and lower values at lower (85-400°C) and higher (800-1020°C) temperatures. Copper has a maximum concentration in vapours at 200-400°C, whereas Mo is most concentrated in vapours at 200-400°C and 600-800°C. Although very little data is available for Y, Au and U, Y appears more concentrated in vapours of medium temperature (400-600°C), whereas Au appears to be preferentially concentrated in vapours of lower temperature, 200-400°C.

Table S3. Compilation of fluid inclusion data

A total of 292 analyses of fluid inclusions from seven porphyry Cu ±Mo ±Au deposits with trace element concentrations and physical phase descriptions (supercritical fluid, brine or vapour inclusions) were compiled from the literature (Fig. 4). The data are from Bajo de la Alumbrera Cu-Au porphyry, Chile (Seo et al., 2009; Ulrich et al, 2001), Bingham Cu-Au-Mo porphyry, USA (Landtwing et al., 2005; Seo et al., 2009), Butte Cu-Mo porphyry, USA (Rusk et al., 2004), El Teniente Cu-Mo porphyry, Chile (Klemm et al., 2007), Famatina Cu-Au porphyry-epithermal, Argentina (Pudack et al., 2009), Rosia-Poieni Cu-Au porphyry, Romania (Kouzmanov et al., 2010) and Santa Rita Cu (Mo) porphyry, New Mexico (Audébat et al., 2008). Only Pb, Cu, Zn and Mo are reported here because S, Cl, Au, REE, Au, U and other elements were almost never reported. The concentrations of Pb, Cu, Zn and Mo were normalized to Na to neutralise the effect of dilution by H₂O and to enable comparison between volcanic vapours and fluid inclusions. The Pb/Na, Cu/Na, Zn/Na and Mo/Na ratios are displayed as violin plots for supercritical fluid-, brine- and vapour inclusions and the ratios for volcanic vapours are displayed beside them.

The Pb/Na ratio is smallest for supercritical fluid inclusions, averaging about 0.006 (note that the calculated averages and the medians shown on violin plots are not necessarily identical), and is progressively higher for vapour and brine inclusions. Volcanic vapours have a large range of Pb/Na values that encompass all the fluid inclusion data and reach values much higher than the latter, averaging around 0.6. The Cu/Na ratios are similar for supercritical fluid and vapour inclusions, with values averaging around 0.8. Brine and volcanic vapours also have similar ratios averaging of 0.03 and 0.05, respectively. The distribution of Zn/Na is very similar to that of Pb/Na; values are smallest for supercritical fluid inclusions, averaging around 0.035, and are gradually higher in vapour and brine inclusions. The Zn/Na ratio reaches a maximum average value of about 0.26 in volcanic vapours, where it also has the greatest range, again encompassing that of most fluid inclusions. Finally, Mo/Na ratios show the highest values (average 0.4) and the greatest variations in volcanic vapors like for Pb/Na and Zn/Na. Vapour, supercritical fluid and brine inclusions have gradually lower Mo/Na ratios ranging between 0.005 and 0.002.

Mass balance calculations

An actively forming porphyry system of intermediate size associated with an overlying volcano that erupts every 5 years would cycle 20,000 times during 100 ka. Assuming an intermediate-sized porphyry deposit containing 1 Gt of Cu, 50 t of Cu should be deposited during each cycle. If 50 wt. % of the Cu present in the basalt is deposited in each cycle, 1.67 Gt of basalt containing 60 ppm Cu (a normal value; see georoc database at georoc.mpch-mainz.gwdg.de/georoc) needs to be injected during each cycle.

Given a density of 2800 kg/m³, this represents a volume of ~ 600 million m³, which is a reasonable size for a mafic injection in the shallow part of subduction zone magma system (Pallister et al., 1992).

Supplementary references

- Audetat, A., Pettke, T., Heinrich, C. A., Bodnar, R. J., 2008. Special paper; The composition of magmatic-hydrothermal fluids in barren and mineralized intrusions. *Economic Geology* 103, 877-908.
- Berlo, K., van Hinsberg, V.J., Vigouroux, N., Gagnon, J.E., Williams-Jones, A.E., 2014. Sulfide breakdown controls metal signature in volcanic gas at Kawah Ijen volcano, Indonesia. *Chemical Geology* 371, 115-127.
- Bernard, A., Symonds R.B., Rose W.I., 1990. Volatile transport and deposition of Mo, W and Re in high temperature magmatic fluids. *Applied Geochemistry* 5, 317-326.
- Camus, G., Gourgaud, A., Mossand-Berthommier, P. C., Vincent, P. M., 2000. Merapi (central Java, Indonesia); an outline of the structural and magmatological evolution, with a special emphasis to the major pyroclastic events. *Journal of Volcanology and Geothermal Research* 100, 139-163.
- Gemmell, J.B., 1987. Geochemistry of metallic trace elements in fumarolic condensates from Nicaraguan and Costa Rican volcanoes. *Journal of Volcanology and Geothermal Research* 33, 161-181.
- Hedenquist, J.W., Aoki, M., Shinohara, H., 1994. Flux of volatiles and ore-forming metals from the magmatic-hydrothermal system of Satsuma Iwojima Volcano. *Geology* 22, 585-588.
- Klemm, L.M., Pettke, T., Heinrich, C. A., Campos, E., 2007. Hydrothermal evolution of the El Teniente Deposit, Chile; porphyry Cu-Mo ore deposition from low-salinity magmatic fluids. *Economic Geology* 102, 1021-1045.
- Kouzmanov, K., Pettke, T., Heinrich, C. A., Bodnar, R., Cline, J., 2010. Direct analysis of ore-precipitating fluids; combined IR microscopy and LA-ICP-MS study of fluid inclusions in opaque ore minerals. *Economic Geology* 105, 351-373.
- Landtwing, M.R., Pettke, T., Halter, W. E., Heinrich, C. A., Redmond, P. B., Einaudi, M. T., Kunze, K., 2005. Copper deposition during quartz dissolution by cooling magmatic-hydrothermal fluids; the Bingham porphyry. *Earth and Planetary Science Letters* 235, 229-243.
- Le Guern, F., Bicocchi P., Nohl A., Tazieff H., 1979. Volcanologie. - Analyse directe des gaz volcaniques. *Comptes-Rendus de l'Académie des Sciences de Paris - Série D* 288, 867-870.
- Le Guern, F., Gerlach, T.M., Nohl, A., 1982. Field gas chromatograph analyses of gases from a glowing dome at Merapi Volcano, Java, Indonesia, 1977, 1978, 1979. *Journal of Volcanology and Geothermal Research* 14, 223-245.
- Menyailov, I.A., Nikitina, L.P., 1980. Chemistry and metal contents of magmatic gases; the new Tolbachik volcanoes case (Kamchatka). *Bulletin Volcanologique* 43, 197-205.
- Mizutani, Y., 1970. Copper and zinc in fumarolic gases of Showashimzan volcano, Hokkaido, Japan. *Geochemical Journal* 4, 87-91.
- Oana, S., 1962. Volcanic gases and sublimes from Showashinzan. *Bulletin of Volcanology* 24, 49-57.
- Pudack, C., Halter, W.E., Heinrich, C.A., Pettke, T., 2009. Evolution of magmatic vapor to gold-rich epithermal liquid; the porphyry to epithermal transition at Nevados de Famatina, northwest Argentina. *Economic Geology* 104, 449-477.
- Ratdomopurbo, A., Beauducel, F., Subandriyo, J., Agung Nandaka, I.G.M., Newhall, C.G., Suharna, Sayudi, D.S., Suparwaka, H., Sunarta, 2013. Overview of the 2006 eruption of Mt. Merapi. *Journal of Volcanology and Geothermal Research* 261, 87-97.
- Rusk, B.G., Reed, M.H., Dilles, J.H., Klemm, L.M., Heinrich, C.A., 2004. Compositions of magmatic hydrothermal fluids determined by LA-ICP-MS of fluid inclusions from the porphyry copper-molybdenum deposit at Butte, MT. *Chemical Geology* 210, 173-199.

- Seo, J.H., Guillong, M., Heinrich, C.A., 2009. The role of sulfur in the formation of magmatic-hydrothermal copper-gold deposits. *Earth and Planetary Science Letters* 282, 323-328.
- Stoiber, R.E., Rose, W.I., 1970. The geochemistry of central american volcanic gas condensates. *Geological Society of America Bulletin* 81, 2891-2912.
- Surono et al., 2012. The 2010 explosive eruption of Java's Merapi volcano—A '100-year' event. *Journal of Volcanology and Geothermal Research* 241-242, 121-135.
- Symonds, R.B., Mizutani, Y., Briggs, P.H., 1996. Long-term geochemical surveillance of fumaroles at Showa-Shinzan Dome, Usu Volcano, Japan. *Journal of Volcanology and Geothermal Research* 73, 177-211.
- Symonds, R.B., Rose W.I., Reed M.H., Lichte F.E., 1987. Volatilization, transport and sublimation of metallic and non-metallic elements in high temperature gases at Merapi Volcano, Indonesia. *Geochimica et Cosmochimica Acta* 51, 2083-2101.
- Symonds, R.B., Rose, W.I., Gerlach, T.M., Briggs, P.H., Harmon, R.S., 1990. Evaluation of gases, condensates, and SO₂ emissions from Augustine Volcano, Alaska; the degassing of a Cl-rich volcanic system. *Bulletin of Volcanology* 52, 355-374.
- Taran, Y.A. et al., 2001. Chemistry and mineralogy of high-temperature gas discharges from Colima Volcano, Mexico; implications for magmatic gas-atmosphere interaction. *Journal of Volcanology and Geothermal Research* 108, 245-264.
- Taran, Y.A., Hedenquist, J.W., Korzhinsky, M.A., Tkachenko, S.I., Shmulovich, K.I., 1995. Geochemistry of magmatic gases from Kudryavy Volcano, Iturup, Kuril Islands. *Geochimica et Cosmochimica Acta* 59, 1749-1761.
- Ulrich, T., Günther, D., Heinrich, C.A., 2001. The evolution of a porphyry Cu-Au deposit, based on LA-ICP-MS analysis of fluid inclusions; Bajo de la Alumbra, Argentina. *Economic Geology* 96, 1743-1774.
- Wahrenberger, C., Seward T.M., Dietrich V., 2002. Volatile trace-element transport in high-temperature gases from Kudryavy volcano (Iturup, Kurile Islands, Russia. In: Wood, R.H. editor, A tribute to A. Crerar. The Geochemical Society, 307-327.
- Zelenski, M., Bortnikova, S., 2005. Sublimate speciation at Mutnovsky Volcano, Kamchatka. *European Journal of Mineralogy* 17, 107-118.

Mineral	Formula	Year	Max	Min
Anglesite	PbSO ₄	2004	470	440
Anhydrite	CaSO ₄	2004	500	225
Arsenic	As	2004	350	190
Barite	BaSO ₄	2004	470	460
Bismuthinite	Bi ₂ S ₃	2006	500	340
Challacolloite	KPb ₂ Cl ₅	2006	560	320
Cotunnite	PbCl ₂	2006	590	300
Fe-Cr alloy	Fe,Cr	2006	590	340
Galena	PbS	2006	560	300
Halite	NaCl	2004, 2006	580	420
Hematite	Fe ₂ O ₃	2004, 2006	600	320
Ilmenite	FeTiO ₃	2004	470	460
Penfieldite	Pb ₂ Cl ₃ (OH)	2004	450	380
Powellite	CaMoO ₄	2004	470	460
Pyrite	FeS ₂	2006	590	300
Salamoniac	NH ₄ Cl	2004	420	190
Smythite	Fe ₉ S ₁₁	2006	480	380
Sulfur	S	2004, 2006	560	190
Sylvite	KCl	2004, 2006	580	440
Tsugaruite	Pb ₄ As ₂ S ₇	2006	340	320
Wurtzite	(Zn,Cd,Fe)S	2006	590	340
Greenockite	CdS	2006	590	340

magmatic system	type	Na	Cu	Zn	Mo	Pb	Reference
Bajo de la Alumbrera Cu-Au porphyry	b	78000	6500			1420	Seo et al., 2009
Bajo de la Alumbrera Cu-Au porphyry	v	24000	1800			210	Seo et al., 2009
Bajo de la alumbrera Cu-Au porphyry	b	160000	7600	14000	70	4500	Ulrich et al., 1999
Bajo de la alumbrera Cu-Au porphyry	v	17000	33000	1200		200	Ulrich et al., 1999
Bajo de la alumbrera Cu-Au porphyry	b	106000	100	6000	140	1700	Ulrich et al., 2002
Bajo de la alumbrera Cu-Au porphyry	b	50000	300	6000		1800	Ulrich et al., 2002
Bajo de la alumbrera Cu-Au porphyry	b	92000	200				Ulrich et al., 2002
Bajo de la alumbrera Cu-Au porphyry	b	105000	100	6000	30	2000	Ulrich et al., 2002
Bajo de la alumbrera Cu-Au porphyry	b	219000	1700				Ulrich et al., 2002
Bajo de la alumbrera Cu-Au porphyry	b	105000	10000	18300	220	4400	Ulrich et al., 2002
Bajo de la alumbrera Cu-Au porphyry	b	243000	3700				Ulrich et al., 2002
Bajo de la alumbrera Cu-Au porphyry	b	252000	2300	20			Ulrich et al., 2002
Bajo de la alumbrera Cu-Au porphyry	b	124000	4800	7400	70	3300	Ulrich et al., 2002
Bajo de la alumbrera Cu-Au porphyry	b	100000	500	8900		2800	Ulrich et al., 2002
Bajo de la alumbrera Cu-Au porphyry	b	107000	1200	12000	120	3600	Ulrich et al., 2002
Bajo de la alumbrera Cu-Au porphyry	b	123000	2200	4600		1600	Ulrich et al., 2002
Bajo de la alumbrera Cu-Au porphyry	b	81000	3200	9500	40	2600	Ulrich et al., 2002
Bajo de la alumbrera Cu-Au porphyry	b	65000	3200	6000	80	1500	Ulrich et al., 2002
Bajo de la alumbrera Cu-Au porphyry	b	198000	1000				Ulrich et al., 2002
Bajo de la alumbrera Cu-Au porphyry	b	80000	5500	9900	90	2400	Ulrich et al., 2002
Bajo de la alumbrera Cu-Au porphyry	b	110000	2600	5400	130	1700	Ulrich et al., 2002
Bajo de la alumbrera Cu-Au porphyry	b	104000	2000	9000	60	2000	Ulrich et al., 2002
Bajo de la alumbrera Cu-Au porphyry	b	100000	5200	5700	50	1800	Ulrich et al., 2002
Bajo de la alumbrera Cu-Au porphyry	b	97000	700	5000		1200	Ulrich et al., 2002
Bajo de la alumbrera Cu-Au porphyry	b	100000	500	1200		1500	Ulrich et al., 2002
Bajo de la alumbrera Cu-Au porphyry	b	33000		1000		200	Ulrich et al., 2002
Bajo de la alumbrera Cu-Au porphyry	b	20000	300	1300		1600	Ulrich et al., 2002
Bajo de la alumbrera Cu-Au porphyry	b	9500	100	200		90	Ulrich et al., 2002
Bajo de la alumbrera Cu-Au porphyry	b	4700		300		110	Ulrich et al., 2002
Bajo de la alumbrera Cu-Au porphyry	v	11000	500				Ulrich et al., 2002
Bajo de la alumbrera Cu-Au porphyry	v	3000	1100	200		70	Ulrich et al., 2002
Bajo de la alumbrera Cu-Au porphyry	v	7000	900	700		200	Ulrich et al., 2002
Bajo de la alumbrera Cu-Au porphyry	v	11000	1200	400		140	Ulrich et al., 2002
Bajo de la alumbrera Cu-Au porphyry	v	3000	300	100		30	Ulrich et al., 2002
Bajo de la alumbrera Cu-Au porphyry	v	6000	3000	300		100	Ulrich et al., 2002
Bajo de la alumbrera Cu-Au porphyry	v	14000	6000	800		170	Ulrich et al., 2002
Bajo de la alumbrera Cu-Au porphyry	v	9800	2500	1000		250	Ulrich et al., 2002
Bajo de la alumbrera Cu-Au porphyry	v	30000	30000	6800		620	Ulrich et al., 2002
Bajo de la alumbrera Cu-Au porphyry	v	13000	29000	1000		40	Ulrich et al., 2002
Bajo de la alumbrera Cu-Au porphyry	v	21000	26000	1300		180	Ulrich et al., 2002
Bajo de la alumbrera Cu-Au porphyry	v	17000	33000	1200		230	Ulrich et al., 2002
Bajo de la alumbrera Cu-Au porphyry	v	7900	5200				Ulrich et al., 2002
Bajo de la alumbrera Cu-Au porphyry	v	3900	1800				Ulrich et al., 2002
Bajo de la alumbrera Cu-Au porphyry	v	3900	500				Ulrich et al., 2002
Bajo de la alumbrera Cu-Au porphyry	v	3900	1700				Ulrich et al., 2002
Bingham Cu-Au-Mo porphyry	b	123000	26000	2900	45	2400	Landtwing et al., 2005
Bingham Cu-Au-Mo porphyry	b	102000	22000	4100	270	3800	Landtwing et al., 2005

Bingham Cu-Au-Mo porphyry	b	108000	15000	2800	94	3800	Landtwing et al., 2005
Bingham Cu-Au-Mo porphyry	b	132000	15000	2700	60	3100	Landtwing et al., 2005
Bingham Cu-Au-Mo porphyry	b	112000	6200	4400		3600	Landtwing et al., 2005
Bingham Cu-Au-Mo porphyry	b	113000	3500	3500	1060	2900	Landtwing et al., 2005
Bingham Cu-Au-Mo porphyry	b	125000	3200	3300	400	3300	Landtwing et al., 2005
Bingham Cu-Au-Mo porphyry	b	110000	2500	4500	70	3700	Landtwing et al., 2005
Bingham Cu-Au-Mo porphyry	b	113000	2100	3800	140	3300	Landtwing et al., 2005
Bingham Cu-Au-Mo porphyry	b	107000	1300	4000	620	4100	Landtwing et al., 2005
Bingham Cu-Au-Mo porphyry	b	123000	700	2100		2100	Landtwing et al., 2005
Bingham Cu-Au-Mo porphyry	b	116000	600	2100		1800	Landtwing et al., 2005
Bingham Cu-Au-Mo porphyry	b	102000	400	3700	44	2900	Landtwing et al., 2005
Bingham Cu-Au-Mo porphyry	b	116000	8100	2500	150	3800	Landtwing et al., 2005
Bingham Cu-Au-Mo porphyry	b	106000	7100	3100	49	3200	Landtwing et al., 2005
Bingham Cu-Au-Mo porphyry	b	980000	6520	3100		3600	Landtwing et al., 2005
Bingham Cu-Au-Mo porphyry	b	105000	4500	3300		2500	Landtwing et al., 2005
Bingham Cu-Au-Mo porphyry	b	115000	3000	2200		2000	Landtwing et al., 2005
Bingham Cu-Au-Mo porphyry	b	960000	2000	3500	21	3200	Landtwing et al., 2005
Bingham Cu-Au-Mo porphyry	b	112000	1450	2100		2600	Landtwing et al., 2005
Bingham Cu-Au-Mo porphyry	b	97000	7600		450	2800	Seo et al., 2009
Bingham Cu-Au-Mo porphyry	b	129000	18900		33	3000	Seo et al., 2009
Bingham Cu-Au-Mo porphyry	b	117000	1190		88	3800	Seo et al., 2009
Bingham Cu-Au-Mo porphyry	v	16800	4200		51	390	Seo et al., 2009
Bingham Cu-Au-Mo porphyry	v	23000	10800		18.3	440	Seo et al., 2009
Bingham Cu-Au-Mo porphyry	v	22000	300		21	540	Seo et al., 2009
Butte Cu-Mo porphyry	b	68000	5900	12000		1200	Rusk et al., 2004
Butte Cu-Mo porphyry	b	110000	170	3300		1000	Rusk et al., 2004
Butte Cu-Mo porphyry	b	100000		5600		1000	Rusk et al., 2004
Butte Cu-Mo porphyry	b	55000		9500			Rusk et al., 2004
Butte Cu-Mo porphyry	b	100000	380	4700		1000	Rusk et al., 2004
Butte Cu-Mo porphyry	b	110000	81	4000		860	Rusk et al., 2004
Butte Cu-Mo porphyry	b	110000	1000	4300		1100	Rusk et al., 2004
Butte Cu-Mo porphyry	b	91000	800	5800		810	Rusk et al., 2004
Butte Cu-Mo porphyry	b	100000	1100	4500		800	Rusk et al., 2004
Butte Cu-Mo porphyry	b	80000	88	6900		1300	Rusk et al., 2004
Butte Cu-Mo porphyry	b	100000	140	8300		1600	Rusk et al., 2004
Butte Cu-Mo porphyry	b	97000	440	12000		2000	Rusk et al., 2004
Butte Cu-Mo porphyry	b	83000	150	9800		1400	Rusk et al., 2004
Butte Cu-Mo porphyry	b	96000	760	15000		1700	Rusk et al., 2004
Butte Cu-Mo porphyry	b	97000		7900		1300	Rusk et al., 2004
Butte Cu-Mo porphyry	b	74000		6400		840	Rusk et al., 2004
Butte Cu-Mo porphyry	b	91000	850	7100	16	1500	Rusk et al., 2004
Butte Cu-Mo porphyry	b	100000	2400	2800		790	Rusk et al., 2004
Butte Cu-Mo porphyry	sc	6300	4400	130		32	Rusk et al., 2004
Butte Cu-Mo porphyry	sc	7800	2100				Rusk et al., 2004
Butte Cu-Mo porphyry	sc	6100	3800	64			Rusk et al., 2004
Butte Cu-Mo porphyry	sc	7800	3400	170	5	20	Rusk et al., 2004
Butte Cu-Mo porphyry	sc	5900	5600	100		8	Rusk et al., 2004
Butte Cu-Mo porphyry	sc	6500	5600	150		24	Rusk et al., 2004

Butte Cu-Mo porphyry	sc	5200	3800	140		10	Rusk et al., 2004
Butte Cu-Mo porphyry	sc	6300	10100	140		35	Rusk et al., 2004
Butte Cu-Mo porphyry	sc	4000	13400	81			Rusk et al., 2004
Butte Cu-Mo porphyry	sc	5100	6600	120		19	Rusk et al., 2004
Butte Cu-Mo porphyry	sc	8900	1100	28			Rusk et al., 2004
Butte Cu-Mo porphyry	sc	6500	6000	100		9	Rusk et al., 2004
Butte Cu-Mo porphyry	sc	8200	1800	160		19	Rusk et al., 2004
Butte Cu-Mo porphyry	sc	6700	2200				Rusk et al., 2004
Butte Cu-Mo porphyry	sc	8100	1500	170			Rusk et al., 2004
Butte Cu-Mo porphyry	sc	8600	1200	150	8	14	Rusk et al., 2004
Butte Cu-Mo porphyry	sc	6900	5000	160		22	Rusk et al., 2004
Butte Cu-Mo porphyry	sc	6600	3600	160		17	Rusk et al., 2004
Butte Cu-Mo porphyry	sc	7800	2300	110		22	Rusk et al., 2004
Butte Cu-Mo porphyry	sc	7900	2200	170		23	Rusk et al., 2004
Butte Cu-Mo porphyry	sc	10000	51	43		30	Rusk et al., 2004
Butte Cu-Mo porphyry	sc	4300	2000	140		11	Rusk et al., 2004
Butte Cu-Mo porphyry	sc	8800	320	100		48	Rusk et al., 2004
Butte Cu-Mo porphyry	sc	5200	2300	100		9	Rusk et al., 2004
Butte Cu-Mo porphyry	sc	6400	160	90		15	Rusk et al., 2004
Butte Cu-Mo porphyry	sc	8200	130	140		58	Rusk et al., 2004
Butte Cu-Mo porphyry	sc	8000	1000				Rusk et al., 2004
Butte Cu-Mo porphyry	sc	7600	1200	100			Rusk et al., 2004
Butte Cu-Mo porphyry	sc	13000		230		76	Rusk et al., 2004
Butte Cu-Mo porphyry	sc	7200	940	190		93	Rusk et al., 2004
Butte Cu-Mo porphyry	sc	9400	600	340		62	Rusk et al., 2004
Butte Cu-Mo porphyry	sc	5700	12000	200		50	Rusk et al., 2004
Butte Cu-Mo porphyry	sc	7000	9900	140			Rusk et al., 2004
Butte Cu-Mo porphyry	sc	5800	10000	460	37	63	Rusk et al., 2004
Butte Cu-Mo porphyry	sc	9100	3100	560	38	83	Rusk et al., 2004
Butte Cu-Mo porphyry	sc	8700	2200	390		48	Rusk et al., 2004
Butte Cu-Mo porphyry	sc	7900	5000	300	343	66	Rusk et al., 2004
Butte Cu-Mo porphyry	sc	6100	7300	240		42	Rusk et al., 2004
Butte Cu-Mo porphyry	sc	10000	360			61	Rusk et al., 2004
Butte Cu-Mo porphyry	sc	6000	12000			77	Rusk et al., 2004
Butte Cu-Mo porphyry	sc	9800		60		26	Rusk et al., 2004
Butte Cu-Mo porphyry	sc	8100	4300	290		46	Rusk et al., 2004
Butte Cu-Mo porphyry	sc	8600	1800	690		63	Rusk et al., 2004
Butte Cu-Mo porphyry	sc	8600	4400	110		52	Rusk et al., 2004
Butte Cu-Mo porphyry	sc	8100	5200			59	Rusk et al., 2004
Butte Cu-Mo porphyry	sc	7100	11000	70		35	Rusk et al., 2004
Butte Cu-Mo porphyry	sc	8300	7900				Rusk et al., 2004
Butte Cu-Mo porphyry	sc	8500	3400	1500		35	Rusk et al., 2004
Butte Cu-Mo porphyry	sc	9700	330	470		100	Rusk et al., 2004
Butte Cu-Mo porphyry	sc	10000				54	Rusk et al., 2004
Butte Cu-Mo porphyry	sc	6500	11000	210		52	Rusk et al., 2004
Butte Cu-Mo porphyry	sc	9600	890	300		88	Rusk et al., 2004
Butte Cu-Mo porphyry	sc	6900	10000	210		44	Rusk et al., 2004
Butte Cu-Mo porphyry	sc	8600	1300	640		81	Rusk et al., 2004

Butte Cu-Mo porphyry	sc	8900	4600		40	Rusk et al., 2004
Butte Cu-Mo porphyry	sc	6200	18000	1600	75	Rusk et al., 2004
Butte Cu-Mo porphyry	sc	7200	12000	300	23	Rusk et al., 2004
Butte Cu-Mo porphyry	sc	7700	13000		42	Rusk et al., 2004
Butte Cu-Mo porphyry	sc	10000	5500			Rusk et al., 2004
Butte Cu-Mo porphyry	sc	7100	15000	210		Rusk et al., 2004
Butte Cu-Mo porphyry	sc	9900	7200	200	100	Rusk et al., 2004
Butte Cu-Mo porphyry	sc	12000	2100			Rusk et al., 2004
Butte Cu-Mo porphyry	sc	9500	8100	330	68	Rusk et al., 2004
Butte Cu-Mo porphyry	sc	4500	18000	350	59	Rusk et al., 2004
Butte Cu-Mo porphyry	sc	6400	14000	270	56	Rusk et al., 2004
Butte Cu-Mo porphyry	sc	7900	8000	1100		Rusk et al., 2004
El Teniente porphyry Cu-Mo	b	96900	820	2600	4	650
El Teniente porphyry Cu-Mo	b	112400	450	2600	11	520
El Teniente porphyry Cu-Mo	b	104600	260	6600	8	2100
El Teniente porphyry Cu-Mo	b	139500	9600	4800	17	760
El Teniente porphyry Cu-Mo	b	92400	4900	4400	12	1000
El Teniente porphyry Cu-Mo	b	86600	2800	4100	55	750
El Teniente porphyry Cu-Mo	b	114200	5000	4300	760	620
El Teniente porphyry Cu-Mo	b	152000	4600	1300	660	460
El Teniente porphyry Cu-Mo	b	159800	7900	1700	1200	610
El Teniente porphyry Cu-Mo	b	200700	3900	1100	830	220
El Teniente porphyry Cu-Mo	b	166200	29100	1400	1300	550
El Teniente porphyry Cu-Mo	b	176400	7400	1300	1000	520
El Teniente porphyry Cu-Mo	b	177600	4200		1800	400
El Teniente porphyry Cu-Mo	b	189700	730		610	610
El Teniente porphyry Cu-Mo	b	97800	400	1700	17	640
El Teniente porphyry Cu-Mo	b	81000	420	2300		460
El Teniente porphyry Cu-Mo	b	75300	400	23700	8	800
El Teniente porphyry Cu-Mo	b	98400	620	910	120	270
El Teniente porphyry Cu-Mo	b	96100	2100	4500	60	1000
El Teniente porphyry Cu-Mo	sc	37800	370	1600	80	220
El Teniente porphyry Cu-Mo	sc	34700	1500	980	6	240
El Teniente porphyry Cu-Mo	sc	5400	1400	220		50
El Teniente porphyry Cu-Mo	sc	8600	3300	240	15	40
El Teniente porphyry Cu-Mo	sc	10200	14400	300	17	50
El Teniente porphyry Cu-Mo	sc	13200	4300	220	8	50
El Teniente porphyry Cu-Mo	sc	5100	21100	110		13
El Teniente porphyry Cu-Mo	sc	15400	4500	150	11	75
El Teniente porphyry Cu-Mo	sc	15500	2500			50
El Teniente porphyry Cu-Mo	sc	14400	2800	250		65
El Teniente porphyry Cu-Mo	sc	11800	6200	270	6	55
El Teniente porphyry Cu-Mo	sc	17300	4600	460	8	75
El Teniente porphyry Cu-Mo	sc	8100	8700	120	7	19
El Teniente porphyry Cu-Mo	sc	20800	1700	190		59
El Teniente porphyry Cu-Mo	v	8800	5800	260	60	35
El Teniente porphyry Cu-Mo	v	900	260	12	6	9
El Teniente porphyry Cu-Mo	v	2900	350	55	3	11

El Teniente porphyry Cu-Mo	v	2200	3200			20	Klemm et al., 2007
El Teniente porphyry Cu-Mo	v	7500	9700	140	3	35	Klemm et al., 2007
El Teniente porphyry Cu-Mo	v	1200	3700				Klemm et al., 2007
El Teniente porphyry Cu-Mo	v	1900	1500	100	4	16	Klemm et al., 2007
El Teniente porphyry Cu-Mo	v	2800	10900	80	8	15	Klemm et al., 2007
El Teniente porphyry Cu-Mo	v	3000	23200	90	5	14	Klemm et al., 2007
El Teniente porphyry Cu-Mo	v	6800	18800	270	19	50	Klemm et al., 2007
El Teniente porphyry Cu-Mo	v	14200	7200	290	55	70	Klemm et al., 2007
El Teniente porphyry Cu-Mo	v	6400	16200	220	25	35	Klemm et al., 2007
El Teniente porphyry Cu-Mo	v	8600	7900		12	60	Klemm et al., 2007
El Teniente porphyry Cu-Mo	v	14400	3200		7		Klemm et al., 2007
Famatina Cu-Au porphyry / HS epitherm b	b	196000	1500		190	1700	Pudack et al., 2009
Famatina Cu-Au porphyry / HS epitherm b	b	128000	880		50	1100	Pudack et al., 2009
Famatina Cu-Au porphyry / HS epitherm b	b	169000	50		40	930	Pudack et al., 2009
Famatina Cu-Au porphyry / HS epitherm b	b	110000	240		360	1200	Pudack et al., 2009
Famatina Cu-Au porphyry / HS epitherm b	b	85000	820		30	940	Pudack et al., 2009
Famatina Cu-Au porphyry / HS epitherm b	b	96000	4600			610	Pudack et al., 2009
Famatina Cu-Au porphyry / HS epitherm b	b	97000	3000			550	Pudack et al., 2009
Famatina Cu-Au porphyry / HS epitherm b	b	114000	3800			540	Pudack et al., 2009
Famatina Cu-Au porphyry / HS epitherm v	v	8000	670		40	90	Pudack et al., 2009
Famatina Cu-Au porphyry / HS epitherm v	v	5000	270		6	60	Pudack et al., 2009
Famatina Cu-Au porphyry / HS epitherm v	v	4000	1100			60	Pudack et al., 2009
Famatina Cu-Au porphyry / HS epitherm v	v	9000	580			70	Pudack et al., 2009
Famatina Cu-Au porphyry / HS epitherm v	v	34000	3300		70	200	Pudack et al., 2009
Famatina Cu-Au porphyry / HS epitherm v	v	8000	2100		20	110	Pudack et al., 2009
Famatina Cu-Au porphyry / HS epitherm v	v	9000	5500			70	Pudack et al., 2009
Famatina Cu-Au porphyry / HS epitherm v	v	7000	390		10	90	Pudack et al., 2009
Famatina Cu-Au porphyry / HS epitherm v	v	7000	1500			90	Pudack et al., 2009
Famatina Cu-Au porphyry / HS epitherm v	v	5000	5400			150	Pudack et al., 2009
Famatina Cu-Au porphyry / HS epitherm v	v	10000	1300			110	Pudack et al., 2009
Famatina Cu-Au porphyry / HS epitherm v	v	1000	440			8	Pudack et al., 2009
Rosia-Poieni porphyry Cu-Au	b	111628	3009	29240		13251	Kouzmanov et al., 2010
Rosia-Poieni porphyry Cu-Au	b	112692	2761	28718		13300	Kouzmanov et al., 2010
Rosia-Poieni porphyry Cu-Au	b	109324	3161	31545		14192	Kouzmanov et al., 2010
Rosia-Poieni porphyry Cu-Au	b	115614	3370	23792		11069	Kouzmanov et al., 2010
Rosia-Poieni porphyry Cu-Au	b	117970	2571	20567		12104	Kouzmanov et al., 2010
Rosia-Poieni porphyry Cu-Au	b	117141	1392	20818		9503	Kouzmanov et al., 2010
Rosia-Poieni porphyry Cu-Au	b	118096	2366	20364		11002	Kouzmanov et al., 2010
Rosia-Poieni porphyry Cu-Au	b	126933	16441	4370		2000	Kouzmanov et al., 2010
Rosia-Poieni porphyry Cu-Au	b	119053	13997	3845		1453	Kouzmanov et al., 2010
Rosia-Poieni porphyry Cu-Au	b	126294	10272	4176		1079	Kouzmanov et al., 2010
Rosia-Poieni porphyry Cu-Au	b	116054	2102	22745		11145	Kouzmanov et al., 2010
Rosia-Poieni porphyry Cu-Au	b	108437	8874	30565		14115	Kouzmanov et al., 2010
Rosia-Poieni porphyry Cu-Au	b	110684	3970	31198		15865	Kouzmanov et al., 2010
Rosia-Poieni porphyry Cu-Au	b	129053	1516	9976		4890	Kouzmanov et al., 2010
Rosia-Poieni porphyry Cu-Au	b	113825	2621	24544		12579	Kouzmanov et al., 2010
Rosia-Poieni porphyry Cu-Au	b	115400	1487	19633		16947	Kouzmanov et al., 2010
Rosia-Poieni porphyry Cu-Au	b	113836	3170	25023		12461	Kouzmanov et al., 2010

Rosia-Poieni porphyry Cu-Au	b	117696	2019	22070	7277	Kouzmanov et al., 2010	
Rosia-Poieni porphyry Cu-Au	b	120260	2314	16677	10056	Kouzmanov et al., 2010	
Rosia-Poieni porphyry Cu-Au	b	118632	1860	18853	10462	Kouzmanov et al., 2010	
Rosia-Poieni porphyry Cu-Au	b	119786		13816	26325	Kouzmanov et al., 2010	
Rosia-Poieni porphyry Cu-Au	b	122163	1885	17538	10794	Kouzmanov et al., 2010	
Rosia-Poieni porphyry Cu-Au	b	119590	1317	21814	11815	Kouzmanov et al., 2010	
Rosia-Poieni porphyry Cu-Au	b	115808	1057	25452	14115	Kouzmanov et al., 2010	
Rosia-Poieni porphyry Cu-Au	b	105602	1748	39610	17722	Kouzmanov et al., 2010	
Rosia-Poieni porphyry Cu-Au	b	97573	2581	43213	20343	Kouzmanov et al., 2010	
Rosia-Poieni porphyry Cu-Au	b	107373	2986	35954	19660	Kouzmanov et al., 2010	
Rosia-Poieni porphyry Cu-Au	b	108885	3725	34765	19574	Kouzmanov et al., 2010	
Rosia-Poieni porphyry Cu-Au	b	109691	5232	34364	18912	Kouzmanov et al., 2010	
Rosia-Poieni porphyry Cu-Au	b	105348	5147	33324	17606	Kouzmanov et al., 2010	
Rosia-Poieni porphyry Cu-Au	b	94639	139	26504	10189	Kouzmanov et al., 2010	
Rosia-Poieni porphyry Cu-Au	b	101573	113	23176	10715	Kouzmanov et al., 2010	
Rosia-Poieni porphyry Cu-Au	b	101142	194	19817	11812	Kouzmanov et al., 2010	
Rosia-Poieni porphyry Cu-Au	b	107724	244	30213	17146	Kouzmanov et al., 2010	
Rosia-Poieni porphyry Cu-Au	b	105114	337	5946	3760	Kouzmanov et al., 2010	
Rosia-Poieni porphyry Cu-Au	b	101035	319	6591	4178	Kouzmanov et al., 2010	
Rosia-Poieni porphyry Cu-Au	b	102399	235	7808	4189	Kouzmanov et al., 2010	
Rosia-Poieni porphyry Cu-Au	b	96803	167	16573	4911	Kouzmanov et al., 2010	
Rosia-Poieni porphyry Cu-Au	v	1675				Kouzmanov et al., 2010	
Rosia-Poieni porphyry Cu-Au	v	1642	30	31	1.7	Kouzmanov et al., 2010	
Rosia-Poieni porphyry Cu-Au	v	1957		24		Kouzmanov et al., 2010	
Rosia-Poieni porphyry Cu-Au	v	1821		3.5		Kouzmanov et al., 2010	
Rosia-Poieni porphyry Cu-Au	v	1961	47		0.5	Kouzmanov et al., 2010	
Rosia-Poieni porphyry Cu-Au	v	1935	1332	33	13	Kouzmanov et al., 2010	
Rosia-Poieni porphyry Cu-Au	v	1963	67			Kouzmanov et al., 2010	
Rosia-Poieni porphyry Cu-Au	v	1567		531	153	Kouzmanov et al., 2010	
Rosia-Poieni porphyry Cu-Au	v	1941		40	0.7	Kouzmanov et al., 2010	
Rosia-Poieni porphyry Cu-Au	v	785		211		Kouzmanov et al., 2010	
Rosia-Poieni porphyry Cu-Au	v	1664		172	33	Kouzmanov et al., 2010	
Rosia-Poieni porphyry Cu-Au	v	1386		134	9.3	Kouzmanov et al., 2010	
Rosia-Poieni porphyry Cu-Au	v	1617		809	23	Kouzmanov et al., 2010	
Rosia-Poieni porphyry Cu-Au	v	1952		28		Kouzmanov et al., 2010	
Rosia-Poieni porphyry Cu-Au	v	1014				Kouzmanov et al., 2010	
Rosia-Poieni porphyry Cu-Au	v	1870			1.4	Kouzmanov et al., 2010	
Rosia-Poieni porphyry Cu-Au	v	1936		4.1	1.5	Kouzmanov et al., 2010	
Rosia-Poieni porphyry Cu-Au	v	1967				Kouzmanov et al., 2010	
Rosia-Poieni porphyry Cu-Au	v	1226		27	15	Kouzmanov et al., 2010	
Rosia-Poieni porphyry Cu-Au	v	1816				Kouzmanov et al., 2010	
Rosia-Poieni porphyry Cu-Au	v	1581	113	76	3.8	Kouzmanov et al., 2010	
Rosia-Poieni porphyry Cu-Au	v	1252	303	832	625	Kouzmanov et al., 2010	
Santa Rita Cu (Mo-u) porphyry	b	67900	2300	3400	800	Audébat et al., 2008	
Santa Rita Cu (Mo-u) porphyry	b	68100	2700	2800	13	590	Audébat et al., 2008
Santa Rita Cu (Mo-u) porphyry	b	75000	2200			780	Audébat et al., 2008
Santa Rita Cu (Mo-u) porphyry	b	74300	2800	2300	42	830	Audébat et al., 2008
Santa Rita Cu (Mo-u) porphyry	b	61800	1700	2800		840	Audébat et al., 2008

Santa Rita Cu (Mo-u) porphyry	b	64900	620		380		Audébat et al., 2008
Santa Rita Cu (Mo-u) porphyry	v	50000	7800	2500	5	410	Audébat et al., 2008
Santa Rita Cu (Mo-u) porphyry	v	50800	8800	1300		390	Audébat et al., 2008
Santa Rita Cu (Mo-u) porphyry	v	28400	4100			200	Audébat et al., 2008
Santa Rita Cu (Mo-u) porphyry	v	50000	3800	1400	15	420	Audébat et al., 2008

